Electronic Supplementary Material (ESI) for Dalton Transactions.

Calcium-intercalated birnessite MnO_2 anchored on carbon nanotubes as high-performance cathodes for aqueous zinc-Ion batteries

Weiwei, Wang,[a] Chi, Zhang, [a] Zhengfan, Chen, [a] Rui, Huang, [a] Yanmei, Nie, [a] Penggao, Liu, [a] Kaiyu, Liu, [a, b]

Jun, Yan* [a c]

Corresponding Authors E-mail：yanjun@csu.edu.cn

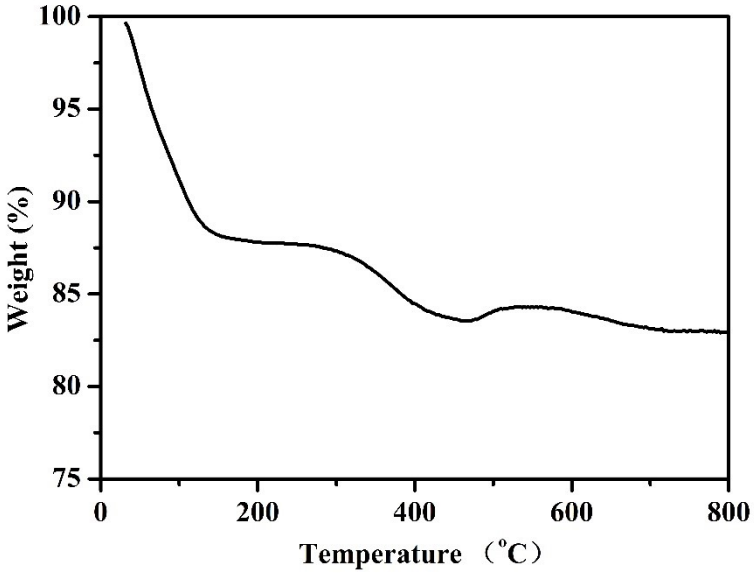

Figure S1. TG curves of CNT-CaMnO composite.

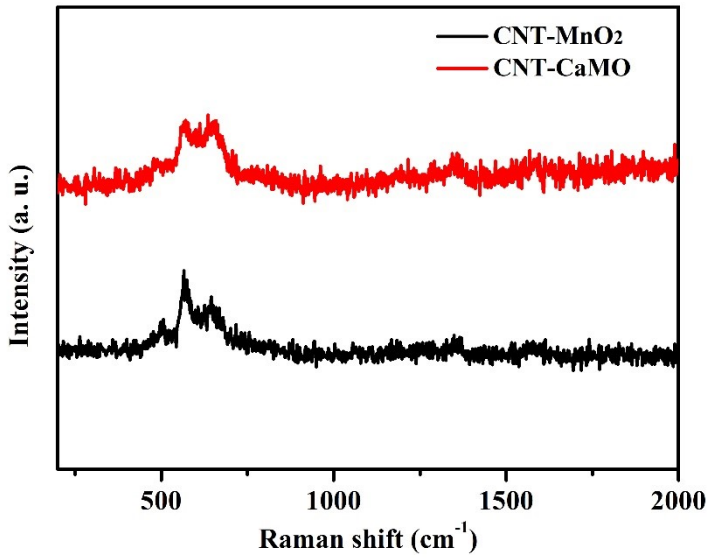

Figure S2. Raman spectra of the CNT-MnO_2 and CNT-CaMO samples.

The two peaks at ~1350 and ~1580 cm^{-1} correspond to the characteristic D-band and G-band of carbon, respectively, where the former comes from the vibrations of disordered carbon and the latter originates from the in-plane C−C bond stretching vibration of graphitic carbon. The band located at ~575 and ~ 636 cm^{-1} as indicated are in agreement with the in-plane Mn−O stretching vibration of MnO_6 groups at the interlayer direction and out-of-plane Mn−O vibration perpendicular to the layers, respectively.

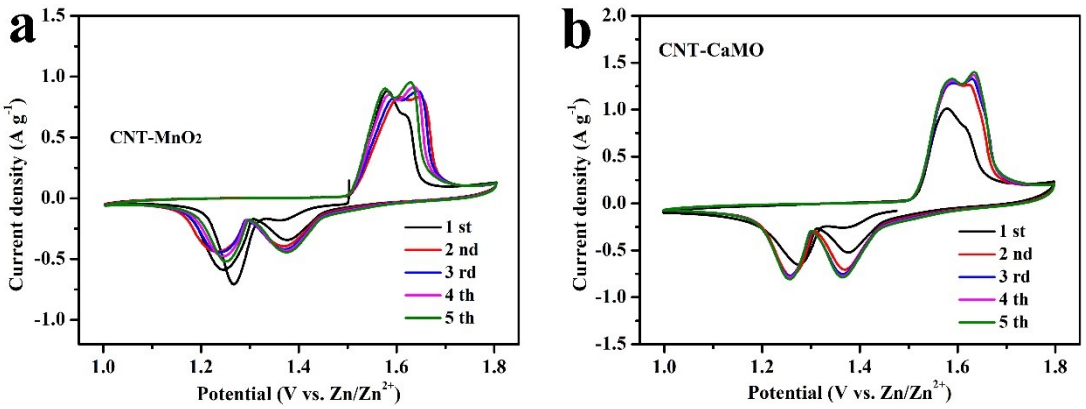

Figure S3. CV curves of the CNT-MnO_2 (a) and CNT-CaMO (b) in initial five cycles.

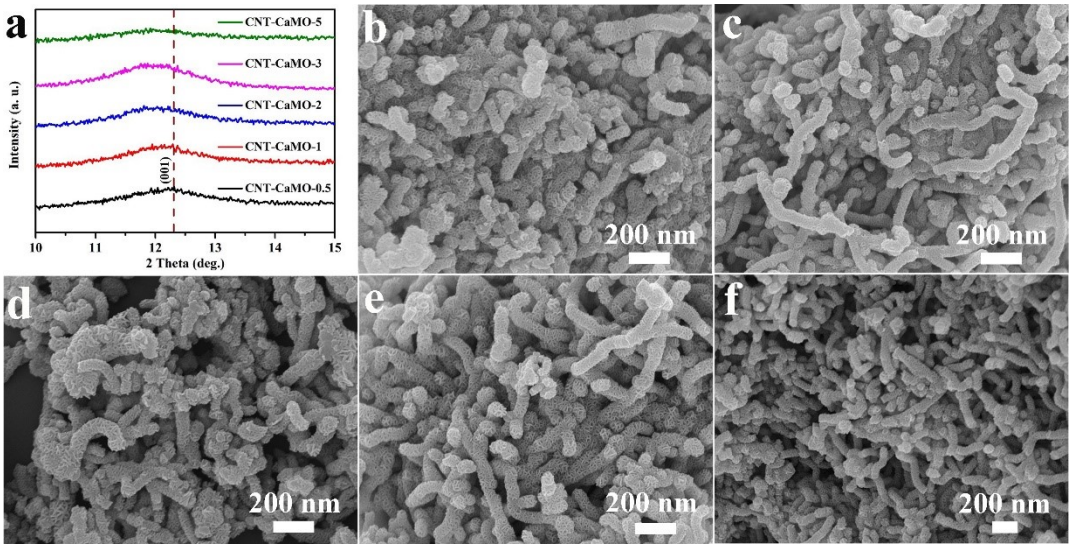

Figure S4. XRD patterns (a), SEM images (b-f) of CNT-CaMO samples with different Ca^{2+} contents.

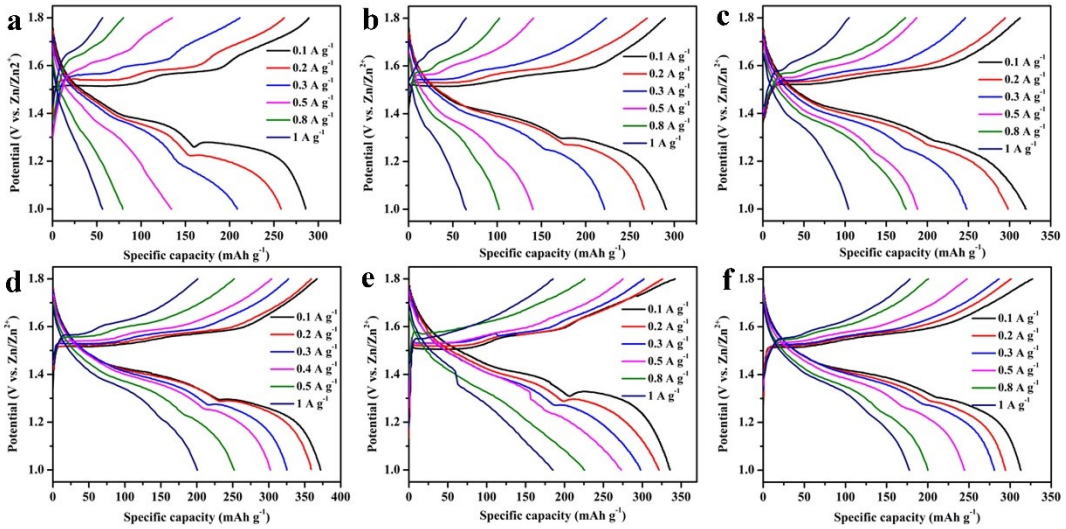

Figure. S5. GCD curves of (a) CNT-MnO_2, (b) CNT-CaMO-0.5, (c) CNT-CaMO-1, (d) CNT-CaMO-2, (e) CNT-CaMO-3, (f) CNT-CaMO-5.

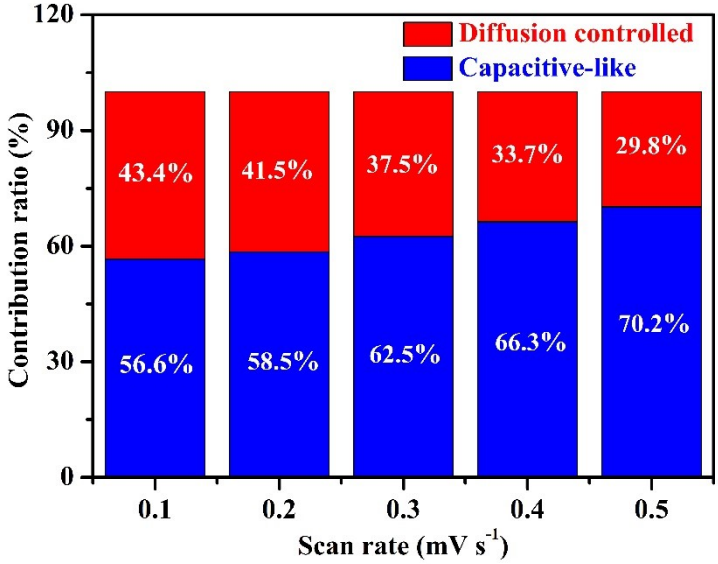

Figure S6. The corresponding percent of pseudocapacitive contribution of CNT-CaMO.

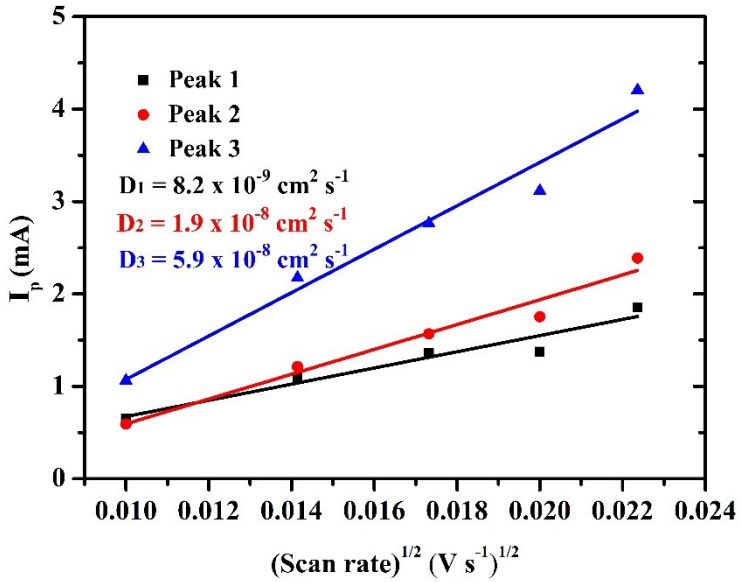

Figure S7. The ions diffusion coefficients of CNT-CaMO by CV measurement.

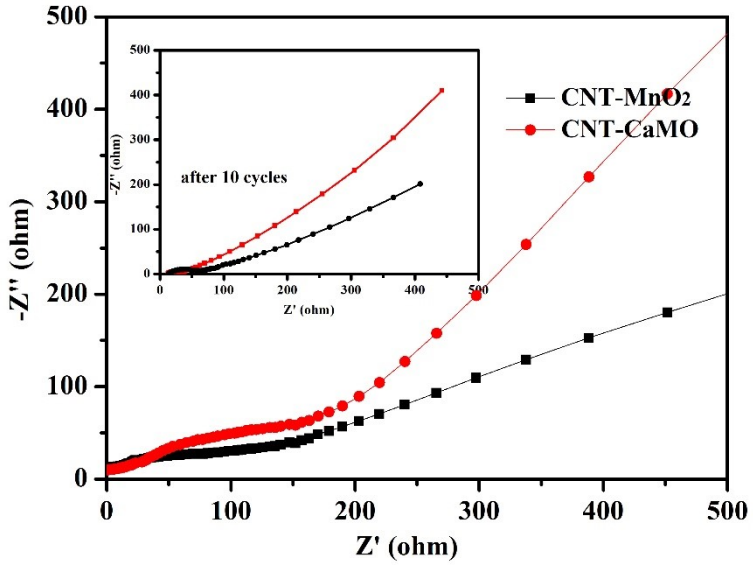

Figure S8. Nyquist plots for CNT-CaMO and CNT-MnO_2 cathodes at initial state and after ten cycles.

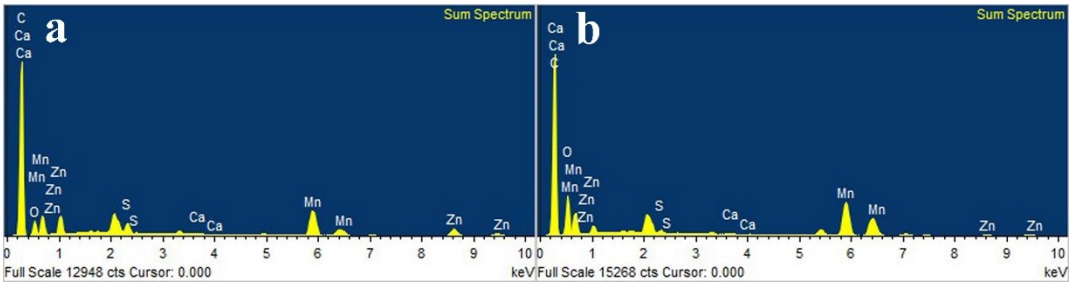

Figure S9. EDS of the fully-discharged (a) and fully-charged electrode (b).

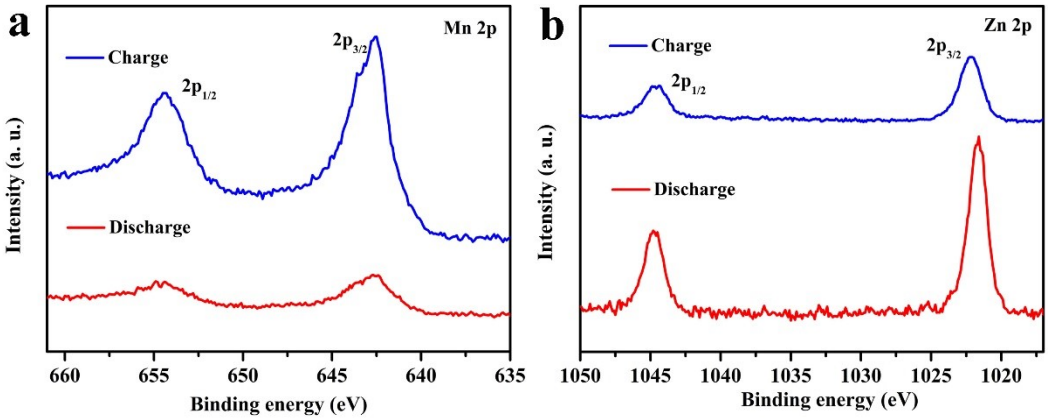

Figure S10. XPS spectra of Mn 2p (a) and Zn 2p (b) at different states.

Table S1. Comparison of cathode performance in aqueous ZIBs between this work and some recent reported manganese-based oxides.

Electrode materials	Electrolyte	Specific capacity	Capacity retention	Ref.
CNT-CaMO	2 M $ZnSO_4$ + 0.2 M $MnSO_4$	351.8 mAh g^{-1} at 200 mA g^{-1}	No obvious capacity fading over 6000 cycles	This work
δ-MnO_2@polyaniline	2 M $ZnSO_4$ + 0.2 M $MnSO_4$	260 mAh g^{-1} at 50 mA g^{-1}	94% retained after 2000 cycles	S2
Graphene Scroll-Coated α-MnO_2	2 M $ZnSO_4$ + 0.2 M $MnSO_4$	362 mAh g^{-1} at 0.3 A g^{-1}	94% retained after 3000 cycles	S3
MnO_2-birnessite	1 M $ZnSO_4$ + 0.2 M $MnSO_4$	266 mA h g^{-1} at 0.1 A g^{-1}	83.7% capacity retention over 2000 cycles	S4
$K_{0.8}Mn_8O_{16}$	2 M $ZnSO_4$+ 0.1 M $MnSO_4$	320 mAh g^{-1} at 100 mA g^{-1}	No obvious capacity fading after 1000 cycles	S5
$Ca_{0.28}MnO_2{\cdot}0.5H_2O$	1 M $ZnSO_4$+ 0.1 M $MnSO_4$	277 mAh g^{-1} at 0.35 A g^{-1}	92% retained after 5000 cycles	S6
Mn-O-3@PPy	2 M $ZnSO_4$ + 0.2 M $MnSO_4$	289.8 mAh g^{-1} at 0.2 A g^{-1}	>100% over 1000 cycles	S7
$ZnMn_2O_4$/N-doped graphene	1 M $ZnSO_4$ + 0.05 M $MnSO_4$	232 mAh g^{-1} at 0.1 A g^{-1}	97.4% over 2500 cycles	S8
Zn-stabilized MnO_2	2 M $ZnSO_4$ + 0.1 M $MnSO_4$	275 mAh g^{-1} at 0.3 A g^{-1}	100% capacity retention over 2000 cycles at 3 A g^{-1}	S9
La^{3+} intercalated δ-MnO_2	1 M $ZnSO_4$ + 0.4 M $MnSO_4$	278.5 mAh g^{-1} at 0.1 A g^{-1}	71% over 200 cycles	S10

Table S2. The weight ratio and atomic of the element of full-discharged electrode.

Element	Weight%	Atomic%
C K	69.46	84.50
O K	11.56	10.55
S K	1.16	0.53
Ca K	0.12	0.04
Mn K	9.91	2.64
Zn K	7.80	1.74
Totals	100.00	

Table S3. The weight ratio and atomic of the element of full-charged electrode.

Element	Weight%	Atomic%
C K	60.75	73.81
O K	24.36	22.22
S K	0.39	0.18
Ca K	0.13	0.05
Mn K	12.68	3.37
Zn K	1.67	0.37
Totals	100.00	

Table S4. The mass concentration based on the ICP-OES.

material	Ca (mg/L)	Mn (mg/L)
CNT-CaMO-0.5	0.918	44.93
CNT-CaMO-1	1.134	45.98
CNT-CaMO-2	1.366	38.68
CNT-CaMO-3	1.79	43.33
CNT-CaMO-5	2.58	42.4

Reference

S1 M. H. Alfaruqi, J. Gim, S. Kim, J. Song, D. T. Pham, J. Jo, Z. Xiu, V. Mathew, J. Kim, *Electrochem. Commun.* 2015, **60**, 121.

S2 J. Huang, Z. Wang, M. Hou, X. Dong, Y. Liu, Y. Wang, Y. Xia, *Nat. Commun.* 2018, **9**, 2906.

S3 B. Wu, G. Zhang, M. Yan, T. Xiong, P. He, L. He, X. Xu, L. Mai, *Small,* 2018, **14**, 1703850.

S4 N. Qiu, H. Chen, Z. Yang, S. Sun, Y. Wang, *Electrochim. Acta*, 2018, **272**, 154−160.

S5 G. Fang, C. Zhu, M. Chen, J. Zhou, B. Tang, X. Cao, X. Zheng, A. Pan, S. Liang, *Adv. Funct. Mater.*, 2019, **29**, 1808375.

S6 T. J. Sun, Q. S. Nian, S.B. Zheng, J. Q. Shi, Z. L. Tao, *Small,* 2020, **16**, 2000597.

S7 A. X. Huang, W. J. Zhou, A. R. Wang, M. F. Chen, J. Z. Chen, Q. H. Tian, J.L. Xu, *Appl. Surf. Sci*. 2021, **545**, 149041.

S8 L. Chen, Z. Yang, H. Qin, X. Zeng, J. Meng, *J. Power Sources*, 2019, **425**. 162-169.

S9 J. Wang, J. G. Wang, H, Liu, C. Wei, F. Kang, *J. Mater. Chem. A*, 2019, **7**, 13727−13735.

S10 H. Zhang, Q. Liu, J. Wang, K. Chen, D. Xue, J. Liu, X. Lu, *J. Mater. Chem. A*, 2019, **7**, 22079-22083.